Goran Pačarek

Assistant J. J. Strossmayer University of Osijek Faculty of Agrobiotechnical Sciences Osijek Croatia

Goran Heffer

Professor J. J. Strossmayer University of Osijek Faculty of Agrobiotechnical Sciences Osijek Croatia

Dejan Marić

Assistant professor University of Slavonski Brod Mechanical Engineering Faculty in Slavonski Brod, Croatia

Ivan Vidaković

Assistant professor J. J. Strossmayer University of Osijek Faculty of Agrobiotechnical Sciences Osijek Croatia

Influence of Sample Speed and Impact Angle on the Wear of Boride Coatings in the Mass of Free Abrasive Particles

This paper presents a study on the wear of boride coatings applied to a C45E steel substrate, tested in the mass of free abrasive particles (Ottawa sand, AFS 50/70), with respect to the sample speed (v) and the impact angle (a) between the abrasive particles and the worn surface. Experimental data were obtained by using a central composite design (CCD) and then statistically processed and analysed. The experimental findings indicate that both the sample speed and the impact angle between abrasive particles and the worn surface are statistically significant factors influencing the wear process and mass loss of the coating, with the speed having a more pronounced effect on mass loss.

Keywords: wear, free abrasive particles, boride coating, impact angle (a), sample speed (v), central composite design (CCD), mass loss

1. INTRODUCTION

Coatings are utilized to enhance material properties, extend the service life of tools, machine components, and structures, and increase the efficiency of manufacturing processes. A wide variety of surface modification techniques exist for this purpose. Carburizing, nitriding, carbonitriding, sulfonitriding, and boriding are processes designed to alter the surface composition of materials [1, 2]. Boriding is a thermo-chemical process in which boron atoms diffuse into the steel surface, chemically bonding with iron from the steel composition to form an iron boride layer. Boride coatings typically exhibit a dual-layer structure, comprising an outer FeB layer and an inner Fe2B layer. The outer FeB layer features an orthorhombic crystal structure, characterized by higher hardness and brittleness, while the inner Fe₂B layer possesses a tetragonal crystal structure, demonstrating relatively lower hardness and improved toughness compared to the FeB layer [3].

The boriding process is conventionally performed at temperatures ranging from 700 to 1000°C for durations of $1{\text -}10\,\text{h}$. Boriding media may be applied in the form of gas, paste, granules, or salt baths [4-6]. The thickness of the boride layer depends on the type of metal substrate, the boriding method, and the process parameters—specifically the temperature and duration of the treatment [7]. The boriding process is applicable to a wide range of materials, including ferrous alloys, nonferrous alloys, and certain superalloys [8]. Boride coatings exhibit hardness values ranging from 1450 to 2100 HV. The thickness of the boride layer depends on the boriding process and typically spans 15–300 μ m, with specific variations based on substrate material: up to 80 μ m for low-carbon steels, up to 150 μ m for

Received: July 2025, Accepted: August 2025 Correspondence to: Goran Pačarek, assistant Faculty of Agrobiotechnical Sciences Osijek, Vladimira Preloga 1, 31000 Osijek, Croatia E-mail: gpacarek@fazos.hr

doi: 10.5937/fme2504558P

medium-carbon steels, and up to 300 µm for cast iron [9-11]. In addition to high hardness, boride coatings are chemically inert and exhibit a low surface friction coefficient, significantly enhancing protection against wear mechanisms such as abrasion, adhesion, galling, and surface fatigue. Alongside their hardness and reduced friction, these coatings provide resistance to corrosion and oxidation while demonstrating hydrophobic properties [1, 3, 12, 13].

Boride coatings find extensive application across numerous industries due to their distinctive properties, including the machinery industry, automotive industry, tooling industry, oil and gas industry, and the agricultural industry [14, 15].

Recent research on boride coatings is focused on improving the process, optimizing the properties of the boride layer, and developing new application methods. Ortiz-Domínguez et al. [15] investigated the growth kinetics of boride coatings formed on steel surfaces using five mathematical mass transfer models, aiming to control the process parameters for coating formation and estimate the boride layer thickness. Medvedovski and Antonov [14] assert that boride coatings significantly enhance the wear resistance of pipes used for transporting petroleum derivatives and sand, demonstrating improved performance against both slurry erosion and dry erosion. Türkmen et al. [16] subjected test specimens of Ti6Al4V alloy to boriding at 1100°C and demonstrated enhanced corrosion resistance and bioactivity, validating their potential for biomedical applications. Türkmen [13] conducted a boriding process on AISI P20 + Ni steel, a material used for manufacturing injection molding dies, and confirmed significant improvements in the mechanical and tribological properties of the boride coating compared to the substrate. Lyalyakin et al. [17] applied highfrequency heating technology to deposit boride coatings using a flux labeled P-0.66 with activators NH₄Cl and CaF₂. The coating process lasted 90–120 seconds, producing layers up to 800 µm thick with microhardness values reaching 2350 HV. Genç et al. [18] investigated and compared various boriding parameters for AISI 1137 steel. Through parameter optimization using the Taguchi method and ANOVA, they validated experimental results and concluded that the boride coating achieved optimal mechanical and tribological properties at a temperature of 950°C and a process duration of 8 h.

The material wear process involves one or a combination of wear mechanisms, including abrasion, galling, adhesion, fatigue, oxidation, and other tribochemical reactions [19-21]. The particle impact angle significantly influences surface wear, defined as the angle between the impacted surface and the direction of the particle's velocity vector. The mass loss rate due to erosive wear is governed by this angle, alongside other particle characteristics such as shape, hardness, dimensions, solid content, velocity, and microstructure [22, 23].

The wear rate is significantly influenced by the type of eroded material, particularly its mechanical properties such as toughness and hardness [24]. Ductile materials typically achieve maximum wear at particle impact angles of 20 - 30°, whereas harder materials exhibit peak wear under perpendicular impacts 90° [25]. Shimizu et al. demonstrated that variations in the particle impact angle significantly influence wear loss in test specimens. Their study further suggests that materials with higher hardness exhibit maximum wear at larger impact angles, aligning with the characteristic brittle fracture behaviour of hard coatings under near-perpendicular impacts [26].

Neilson and Gilchrist [27] tested the impact of aluminium oxide particles at varying angles on aluminium, glass, perspex, and carbon plates. They developed an equation correlating the wear rate with the particle impact angle, establishing a quantitative framework for predicting erosive wear in diverse materials. Additionally, Oka et al. [28] proposed a universal formula for material wear at specific particle impact angles, and while numerous researchers have developed equations to predict wear rates, no practical and efficient equation has yet been established for material degradation in industrial plants. Current models often fail to account for dynamic industrial conditions, material-specific properties (e.g., hardness, microstructure), and mixed wear mechanisms, necessitating customized solutions for applications like boride coatings in high-wear environments [29]. Oka et al. report that particle velocity solely increased material wear and did not influence the dependence of the impact angle on wear for metallic materials. This observation underscores the distinct roles of kinetic energy (governed by velocity) and impact geometry in erosive processes. Oka et al. [23] emphasize that hardness, as a mechanical property of materials, is one of the most critical parameters in developing equations for estimating wear under any particle impact angle. Given the complexity of factors influencing surface wear (e.g., particle velocity, shape, microstructure), experimentally investigating each variable's effect and erosion mechanisms would be prohibitively costly and time-intensive. This challenge can be mitigated through numerical simulation, which offers a flexible framework to model the intricate interactions governing surface degradation [30].

Among the pioneers in applying two-dimensional numerical models for single-particle impact simulations are Shimizu et al. [26, 31] and Chen and Li [32]. Technological and computational advancements have enabled the development of sophisticated 3D models capable of simulating single impacts of both spherical and angular particles [33-35]. However, traditional single-particle simulations fail to capture the cumulative effects of multiple particles impacts on a surface. To address this limitation, a novel 3D dynamic model has been developed, incorporating multiple factors (e.g., particle distribution, velocity gradients, material anisotropy) to better replicate real-world erosion processes [36]. Jafari and Hattani [21] applied the Discrete Element Method (DEM) to model material wear under particle impact. The DEM approach involves solving equations of motion to determine the position, velocity, and acceleration of all particles in the system.

This work aims to advance research on wear of boride coatings caused by movement through free abrasive particles, specifically investigating the effects of sample speed and impact angle on wear mechanisms. In order to examine the combined influence of abrasive and erosive wear, a testing approach was implemented that enables the simultaneous assessment of both mechanisms, as opposed to standardized methods that generally permit the evaluation of each mechanism independently. By moving in the mass of free abrasive particles, the surface of the material is simultaneously worn by the mechanisms of abrasion and erosion, which is described as a transition from abrasive sliding wear to particle erosion wear [37, 38]. Consequently, the term "abrasive erosion" can be used. This type of wear is not investigated a lot, what can be the novelty of this work.

In addition, the achieved results enable the optimization of protective materials for industrial applications where abrasive erosion resistance is critical, such as oil delivery pipes and pumping systems in heavy oil extraction from wells and oil sand processing, agricultural tools, earthmoving and transportation equipment, quarry grinders, cement mills, grain transport mechanisms and parts, parts in the brick industry and tillage equipment [39-41].

2. MATERIALS AND METHODS

2.1 Samples for experiment

Test samples were fabricated as 40mm × 2 mm × 5mm plates using C45E medium-carbon steel (EN) as the substrate material. Prior to boriding, the samples were finely ground with 2000-grit abrasive paper to ensure uniform surface conditions. The chemical composition of the substrate was determined via optical emission spectrometry (OES), while microstructural analysis of the coating was conducted using a Tescan Vega TS5136LS scanning electron microscope (SEM) equipped with energy-dispersive X-ray spectroscopy (EDS). Chemical composition of substrate is: C 0.46 %, Si 0.29 %, Mn 0.69 %, P 0.026 %, S 0.029 %, Cr 0.024 %, Mo 0.08 %, Ni 0.02 and Fe balanced. Surface and cross-sectional microhardness measurements were

performed using a Shimadzu HMW-2T Vickers microhardness tester.

The test samples were borided using the commercial boriding powder Ekabor 3 at $1000\,^{\circ}\text{C}$ in a chamber furnace for 4 h, followed by air cooling. The microstructure of the resulting boride coating is illustrated in Figure 1, revealing the characteristic dual-layer structure of FeB (outer) and Fe₂B (inner) phases.

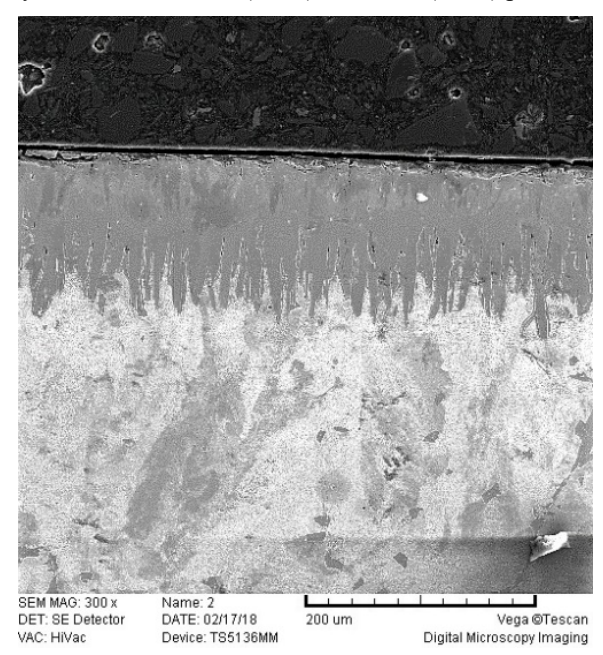


Figure 1. SEM micrograph of the boride sample

Figure 1 shows the good indentation of the boride coating into the substrate material and the relatively compact structure of the coating. The thickness of the resulting boride coating is 65-135 μ m, and the average measured hardness is 1320 HV0.2. The substrate material has an average measured hardness of 270 HV0.2. The microstructure of the coating obtained by boriding and subsequently etched in the nital is shown in Figure 2.

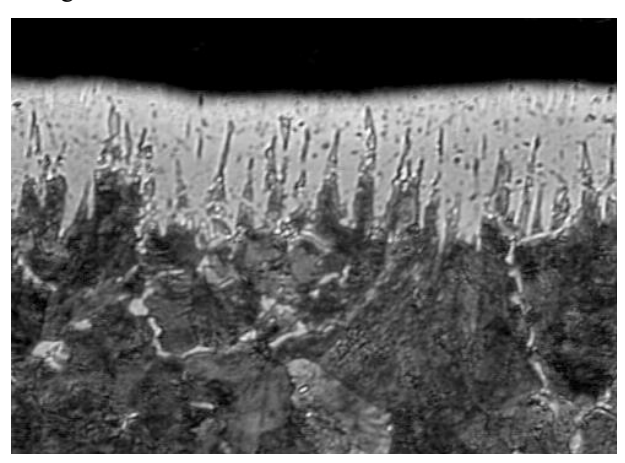
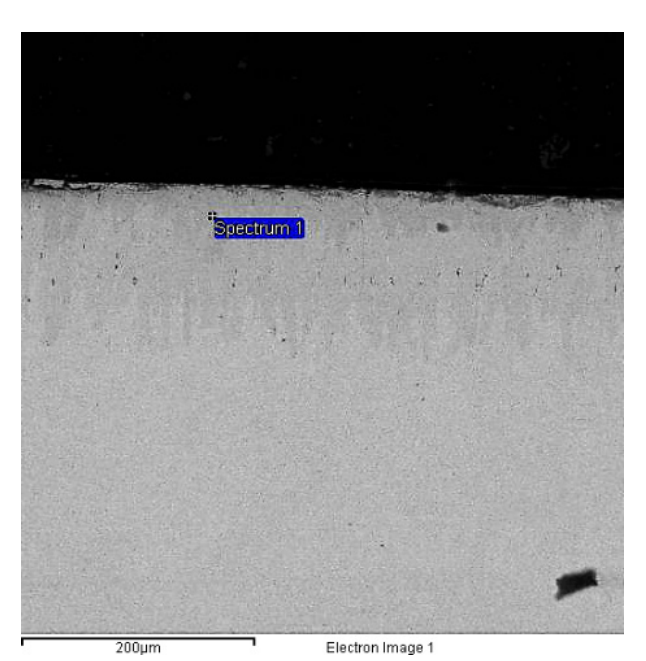


Figure 2. Microstructure of the boride sample

The Figure 2 confirms a good quality of the boride coating. Figure 3 shows the EDS analysis of the boride coating in a given point/area (Spectrum 1).

The results of EDS analysis in Figure 3 show that the boride coating is composed of 19.54% B, 6.06% C and 74.40% Fe.



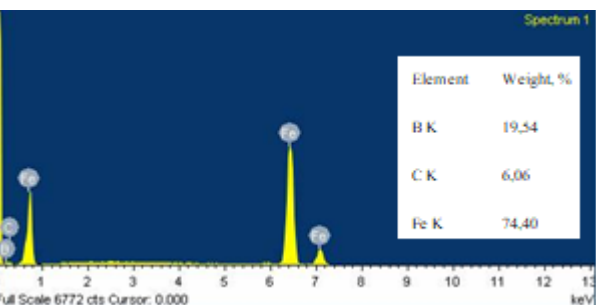


Figure 3. EDS analysis of the boride coating at the specified point/region (Spectrum 1)

2.2 Wear experiment

The wear test was performed in the mass of free abrasive particles, i.e. sand using the device shown in Figure 4. The test was performed using Ottawa AFS 50/70 rounded quartz sand, with a grain size between 212 μ m and 300 μ m. The test device has a diameter of 1000 mm and a depth of 400 mm with an abrasive capacity of up to 300 kg [42]. The device allows:

- application of different abrasives
- testing of different coatings
- changing the test sample holder
- variation of the test sample speed in the range from 0.5 m/s to 3.5 m/s
- variation of the impact angle of the abrasive particle from 0° to 90° (Figure 5)
- test repeatability.

For the processing and analysis of experimental data, a central composite design (CCD) was applied to provide a qualitative analysis of the individual and interaction effects of input variables [43]. According to the central composite design, for each coating wear test, minimum and maximum input variables and four replicates were defined at the central point of the experiment. The test input variables are:

v – sample speed in the range from 1 to 3 m/s

 α – impact angle of abrasive particles with the coating in the range from 0° to 90° .

The experimental output is the material wear $[\Delta m]$, expressed as the mass loss of the samples [g] after the wear test procedure. The total wear distance was 50000 m.

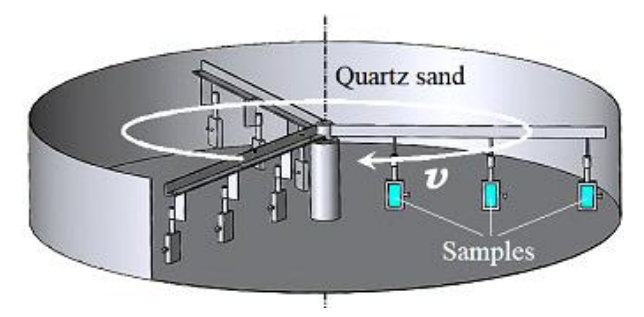


Figure 4. Schematic diagram of the sample wear device [42]

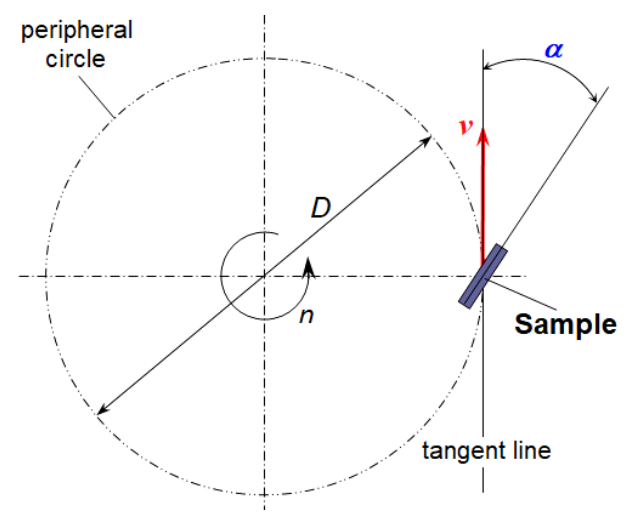


Figure 5. Schematic representation of placing the test sample at a certain angle [42]

The sample holders, immersed in a container of abrasive medium, were adjustable to specific impact angles (α) between the abrasive particles and the worn surface.

The tangential speed (v) of the test samples was determined by the holder's position on the pitch circle (Figure 5). The holder rotated at 66 min⁻¹, exposing only one surface to abrasive particle impacts during testing.

The remaining surfaces were shielded from abrasion and served as clamping interfaces for screw fixation and sample stabilization.

The mass loss of test samples and boride coatings after wear was measured using a Mettler B5C 1000 analytical balance with a precision of 10^{-4} g. The

difference in the measured masses of the test samples before and after the wear process was determined, which represented the mass loss of the tested samples. The preparation procedure for each test sample was carried out in such a way that the test sample was thoroughly rinsed under a stream of water in order to remove fine particles and dried with warm air.

3. RESULTS AND DISCUSSION

Analysis of the wear results of the test samples was performed using the Design Expert software. The measured mass losses of the boride coating samples according to the CCD experiment are given in Table 1.

Table 1. Wear results

Run	Factor A:	Factor B:	Response:	
	Sample speed	Impact angle	Mass loss	
	(m/s)	(degree)	$(<10^{-4} \text{ g})$	
1.	2.00	45.00	40	
2.	1.00	90.00	18	
3.	1.00	0.00	28	
4.	0.59	45.00	31	
5.	3.00	90.00	87	
6.	2.00	45.00	37	
7.	2.00	-18.64	25	
8.	2.00	45.00	32	
9.	2.00	108.64	11	
10.	3.00	0.00	112	
11.	3.41	45.00	165	
12.	2.00	45.00	39	

The experimental results of the investigation of boride coatings were processed using the analysis of variance (ANOVA), which determines the significance of the observed factors in the wear process based on p-value

Table 2 shows the results obtained by ANOVA for the quadratic statistical model.

The accuracy of the proposed second-order response surface model was confirmed with a p - value of 0.0001, which confirms the statistically significant difference of the selected model describing the wear process. In the observed case, the factors of sample speed $(A,\,A^2)$ and impact angle $(B,\,B^2)$ affect wear, while the interaction of variables (AB) is not significant. The suitability of the model was assessed by the coefficient of determination $R^2=0.9890$, which confirms the good fit of the model.

Table 2. ANOVA for quadratic model

Source	Sum of	Degrees of	Mean	F-Value	p-Value	
	Squares	Freedom	Square			
Model	22860.33	5	4572.07	107.75	< 0.0001	significant
A – Sample speed	14663.68	1	14663.68	345.59	< 0.0001	
B – Impact angle	375.37	1	375.37	8.85	0.0248	
AB	56.25	1	56.25	1.33	0.2934	
A^2	6275.03	1	6275.03	147.89	< 0.0001	
B^2	483.03	1	483.03	11.38	0.0150	
Residual	254.58	6	42.43			
Lack of Fit	216.58	3	72.19	5.70	0.0934	not significant
Pure Error	38.00	3	12.67			
Cor Total	23114.92	11				

The mathematical model for the wear process of boride coatings in terms of actual variables was derived as a regression equation (1):

$$\Delta m = 67.28662 - 78.68692 \cdot v + 0.40056 \cdot \alpha -$$

$$-0.083333 \cdot v \cdot \alpha + 31.31250 \cdot v^2 - 4.29012 \cdot 10^{-3} \cdot \alpha^2$$
 (1)

The wear model for the boride coating is defined as a second-order polynomial with a high coefficient of determination. The derived mathematical model of boride coating wear is graphically represented by a 3D response surface diagram (Figure 6), showing the effects of the variables (sample speed and impact angle of the abrasive particle) on the wear result (mass loss).

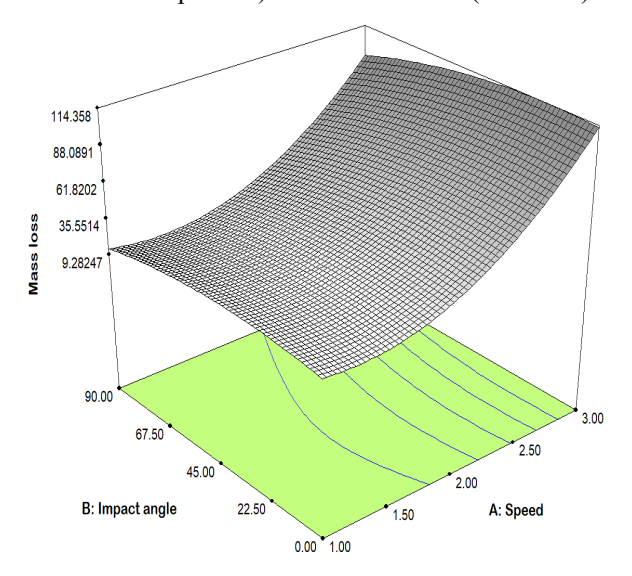


Figure 6. Response surface diagram of the mass loss (impact angle, $^{\circ}$, speed, m/s, mass loss, \cdot 10⁻⁴ g)

From the 3D response surface diagram shown in Figure 6, it can be seen that the mass loss increases (exponentially) with increasing speed from 1 m/s to 3 m/s. Similar results were shown in [21, 24, 42]. Accordingly, all tested samples (depending on the impact angle) had the highest mass loss at the highest sample speed (3 m/s). The increase in the wear rate, or the mass loss, with increasing speed occurs because the kinetic energy of the impact of abrasive particles on the worn surface increases, which plays a key role in the wear mechanism, since in the calculation of kinetic energy, speed participates with a square exponent.

Comparing the same sample speeds of the impacting particle and two different particle impact angles (α) at 0° and 90° as shown in Figure 7, the greatest wear will be at the angle of 0°.

The diagram in Figure 6 shows that the mass loss of the boride coating is influenced by the impact angle (α) of the tested sample as well. Comparing the impact angles α (0° and 90°) and the wear-related mass loss, it can be seen that the smaller the impact angle of the abrasive particle and the worn surface, i.e. the closer it is to 0°, the greater the mass loss, as shown in Figure 7.

With an increase in the impact angle, the mass loss increases only very slightly up to an impact angle of 45°; with a further increase in the impact angle, the mass loss decreases, whereby it is lowest at the largest impact angle of 90°. The greater mass loss as a function of the impact angle is more pronounced at higher

sample speeds. The greater mass loss at a lower impact angle can be related to the duration of contact between the abrasive particle and the worn surface when considering the single case, i.e. the contact of an abrasive particle with the worn surface. With a smaller impact angle, the abrasive particles remain in contact with the worn surface for longer, as they continue to slide on the surface after the impact and thus cause a greater mass loss. At a higher impact angle, the abrasive particles are repelled after the impact and thus reduce the contact with the worn surface, so that the mass loss is smaller.

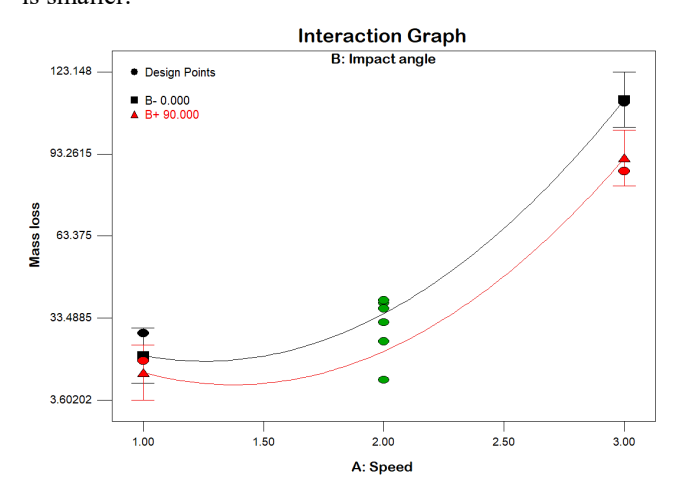


Figure 7. Interaction graph between sample speed and impact angle (impact angle, °, speed, m/s, mass loss, · 10⁻⁴ g)

4. CONCLUSION

The experiment conducted in this study demonstrated that the tested boride coatings exhibit high resistance to wear in the mass of free abrasive particles, attributed primarily to their exceptional hardness. Microhardness measurements revealed that the boride coating had an average hardness 4.88 times greater than the substrate. Over a total wear distance of 50.000 metres, the boride coating had a greater mass loss at lower impact angles (up to 45°) and at higher sample speeds (around 3 m/s), while the boride coating had a lower mass loss at higher impact angles (around 90°) and at lower sample speeds (around 1 m/s).

Statistical analysis of the wear test results confirmed that sample speed (v) and particle impact angle (α) significantly influence the wear process, where sample speed has a greater influence on mass loss than the impact angle.

A second-order polynomial response surface model was derived to describe the wear behaviour of the boride coating. The model's accuracy was validated through ANOVA tests and a high coefficient of determination R², demonstrating strong agreement between experimental data and model predictions.

ACKNOWLEDGMENT

This research was supported by the project "Application of modern technologies and additional materials with the aim of extending the life of working parts of agricultural machinery" from the research team "Technical and technological systems in agriculture,

GIT, precision agriculture and environment protection" of the Faculty of Agrobiotechnical Sciences Osijek.

REFERENCES

- [1] Petrova, R.S., Suwattananont, N. and Samardzic, V.: The effect of boronizing on metallic alloys for automotive applications, J. Mater. Eng. Perform, Vol. 17, pp. 340-345, 2008.
- [2] Attarzadeh, N., Molaei, M., Babaei, K. and Fattahalhosseini, A.: New promising ceramic coatings for corrosion and wear protection of steels: a review, Surf. Interfaces, Vol. 23, 100997, 2021.
- [3] Panda, J.N., Wong, B.C., Medvedovski, E. Egberts, P.: Enhancement of tribo-corrosion performance of carbon steel through boronizing and BN-based coatings, Tribol. Int, Vol. 153, 106666, 2021.
- [4] Matijević, B.: *Kinetika difuzijskog stvaranja kar-bidnih slojeva*, PhD thesis, Faculty of Mechanical Engineering and Naval Architecture, University of Zagreb, Zagreb, 1997.
- [5] Sen, S., Sen, U. and Bindal, C.: An Approach to Kinetic Study of Borided Steels, Surf. Coat. Technol, Vol. 191, No. 2-3, pp. 274-285, 2005.
- [6] Novakova, A., Sizov, I., Golubok, D.S., Yu Kiseleva, T. and Revokatov, P.: Electron-Beam Boriding of Low-Carbon Steel, J. Alloy Comp, Vol. 383, No. 1-2, pp. 108-112, 2004.
- [7] Chatterjee Fisher, R.: Boriding and diffusion metallizing. In: Sudarshan, T.S. (ed.). Surface Modification Technologies, An Engineer's Guide, Marcel Dekker, New York, pp. 567-609, 1989.
- [8] Jain, V. and Sundararajan, G.: Influence of the pack thickness of the boronizing mixture on the boriding of steel, Surf. Coat. Tech, Vol. 149, No. 1, pp. 21-26, 2002.
- [9] Morales-Robles, Á.J., Ortiz-Domínguez, M., Gómez-Vargas, O.A. and Moreno-González, M.D.l.L.: Boronize Coatings Studied with a New Mass Transfer Model, Mater, Vol. 17, No. 21, 5309, 2024.
- [10] Meric, C., Sahin, S., Backir, B. and Koksal, N.S.: Investigation of the boronizing effect on the abrasive wear behavior in cast irons, Mater. Des, Vol. 27, No. 9, pp. 751-757, 2006.
- [11] Fischer, S.F., Muschna, S., Bührig-Polaczek, A. and Bünck, M.: In-situ surface hardening of cast iron by surface layer metallurgy, Mater. Sci. Eng. A, Vol. 615, pp. 61-69, 2014.
- [12] Yönetken, A., Erol, A.: Investigation of mechanical properties of boronized composites produced by electroless Ni coating, JoMME, Vol. 6, pp. 1-6, 2020.
- [13] Türkmen, İ.: Enhancing surface properties of AISI P20 + Ni mold steel via boronizing: Evaluation of mechanical, tribological, and corrosion performance, J. Mater. Sci, Vol. 59, pp. 21102-21128, 2024.
- [14] Medvedovski, E. and Antonov, M.: Erosion studies of the iron boride coatings for protection of tubing components in oil production, mineral processing

- and engineering applications, Wear, Vol. 452-453, 203277, 2020.
- [15] Ortiz-Domínguez, M., Morales-Robles, Á.J., Gómez-Vargas, O.A. and Moreno-González, G.: Surface Growth of Boronize Coatings Studied with Mathematical Models of Diffusion, Metals, Vol. 14, 670, 2024.
- [16] Türkmen, İ., Kanbur, K. Sargin, F.: Characteristics of boronized Ti6Al4V alloy using boric acid based boronizing mixture, Mater. Charact, Vol. 192, 112180, 2022.
- [17] Lyalyakin, V.P., Aulov, VF., Ishkov, AV., Kravchenko, I.N. and Kuznetsov, Y.A.: Properties of wear-resistant composite coatings produced by high-speed boronizing, J. Mach. Manuf. Reliab, Vol. 51, pp. 134-142, 2022.
- [18] Genç, A., Urtekin, L. Danimaz, M.: Characterization and Optimization of Boride Coatings on AISI 1137 Steel: Enhancing Surface Properties and Wear Resistance, Coat, Vol. 15, No. 1, 10, 2024.
- [19] Zhai, W., Bai, L., Zhou, R., Fan, X., Kang, G., Liu, Y. and Zhou, K.: Recent progress on wear-resistant materials: designs, properties, and applications, Adv. Sci, Vol. 8, 2003739, 2021.
- [20] Chintha, A.R., Valtonen, K., Kuokkala, V.T., Kundu, S., Peet, M.J. and Bhadeshia, H.K.D.H.: Role of fracture toughness in impact-abrasion wear, Wear, Vol. 428-429, pp. 430-437, 2019.
- [21] Jafari, A. and Abbasi Hattani, R.: Investigation of parameters influencing erosive wear using DEM, Friction, Vol. 8, pp. 136-150, 2020.
- [22] Doubek, P., Filípek, J.: Abrasive and erosive wear of technical materials, Acta Univ. Agric. Silvic. Mendel. Brun, Vol. 59, No. 3, pp. 13-21, 2011.
- [23] Oka, Y.I., Mihara, S., Yoshida, T.: Impact-angle dependence and estimation of erosion damage to ceramic materials caused by solid particle impact, Wear, Vol. 267, pp. 129-117, 2009.
- [24] Kosa, E., Göksenli, A.: Effect of impact angle on erosive abrasive wear of ductile and brittle materials, Int. J. Mech. Mechatron. Eng, Vol. 9, No. 9, pp. 1638-1642, 2015.
- [25] Nandre, B.D., Desale, G.R.: Study the effect of impact angle on slurry erosion wear of four different ductile materials, Mater. Today Proc, Vol. 5, No. 2, pp. 7561-7570, 2018.
- [26] Shimizu, K., Noguchi, T., Seitoh, H. and Muranaka, E.: FEM analysis of the dependency on impact angle during erosive wear, Wear, No. 233-235, pp. 157-159, 1999.
- [27] Neilson, J.H., Gilchrist, A.: Erosion by a stream of solid particles, Wear, Vol. 11, No. 2, pp. 111-122, 1968.
- [28] Oka, Y.I., Ohnogi, H., Hosokawa, T. Matsumura, M.: The impact angle dependence of erosion damage caused by solid particle impact, Wear, Vol. 203-204, pp. 573-579, 1997.
- [29] Sundararajan, G.: The solid particle erosion of metallic materials: the rationalization of the influence

- of material variables, Wear, Vol. 186, No. 1, pp. 129-144, 1995.
- [30] Yaer, X., Shimizu, K., Qu, J., Wen, B., Cao, X. Kusumoto, K.: Surface deformation micromechanics of erosion damage at different angles and velocities for aero-engine hot-end components, Wear, Vol. 426-427, Part A, pp. 527-538, 2019.
- [31] Shimizu, K., Noguchi, T., Seitoh, H., Okada, M. and Matsubara, Y.: FEM analysis of erosive wear, Wear, Vol. 250, No. 1-12, pp. 779-784, 2001.
- [32] Chen, Q., Li, D.Y.: Computer simulation of solid-particle erosion of composite materials, Wear, Vol. 255, No. 1-6, pp. 78-84, 2003.
- [33] Molinari, J.F., Ortiz, M.: A study of solid-particle erosion of metallic targets, Int. J Impact Eng, Vol. 27, No. 4, pp. 347-178, 2002.
- [34] Woytowitz, P.J., Richman, R.H.: Modeling of damage from multiple impacts by spherical particles, Wear, Vol. 233-235, pp. 120-133, 1999.
- [35] Lari, M.S., Papini, M.: Inverse methods to gradient etch three-dimensional features with prescribed topographies using abrasive jet micro-machining: Part I–Modeling, Precis. eng, Vol. 45, pp. 272-284, 2016.
- [36] Zheng, C., Liu, Y., Chen, C., Qin, J., Ji, R., Cai, B.: Numerical study of impact erosion of multiple solid particle, Appl. Surf. Sci, Vol. 423, pp. 176-184, 2017.
- [37] Franek, F., Badisch, E., Kirchgaßner, M.: Advanced methods for characterisation of abrasion/erosion resistance of wear protection materials, FME Transactions, Vol. 37, No. 2, pp. 61-70, 2009.
- [38] Sommer, K., Heinz, R., Schöfer, J.: Verschleiß metallischer Werkstoffe, Erscheinungsformen sicher beurteilen, Springer Vieweg, 2014.
- [39] Heffer, G., Samardžić, I., Schauperl, Z., Vidaković, I.: Wear of Induction Cladded Coating in the Abrasive Mass at Various Speeds and Impact

- Angles, Tehnički vjesnik-Technical Gazette, Vol. 25, No. 6, pp. 1776-1782, 2018.
- [40] Malvajerdi, A.S.: Wear and coating of tillage tools: A review, Heliyon, Vol. 9, No. 6, e16669, 2023.
- [41] Medvedovski, E., Leal Mendoza, G., Vargas, G.: Influence of Boronizing on Steel Performance under Erosion-Abrasion-Corrosion Conditions Simulating Downhole Oil Production, Corrosion and Materials Degradation, Vol. 2, No. 2, pp. 293-324, 2021.
- [42] Heffer, G., Šimunović, K., Samardžić, I., Vidaković, I.: Effect of Speed and Impact Angle on Solid Particle Erosion of Vanadium Carbide Coatings Produced by Thermo-Reactive Diffusion Technique, FME Transactions, Vol. 48, No. 3, pp. 497-503, 2020.
- [43] Montgomery, D.C.: *Design and Analysis of Experiments*, Eighth Edition, John Wiley & Sons, Inc., Hoboken, 2013.

УТИЦАЈ БРЗИНЕ УЗОРКА И УГЛА УДАРА НА ХАБАЊЕ БОРИДНИХ ПРЕМАЗА У МАСИ СЛОБОДНИХ АБРАЗИВНИХ ЧЕСТИЦА

Г. Пачарек, Г. Хефер, Д. Марић, И. Видаковић

Овај рад представља студију о хабању боридних премаза нанетих на подлогу од челика С45Е, тестирану у маси слободних абразивних честица (Отава песак, AFS 50/70), у односу на брзину узорка (v) и угао удара (a) између абразивних честица и истрошене површине. Експериментални подаци су добијени коришћењем централног композитног дизајна (ССD), а затим статистички обрађени и анализирани. Експериментални налази указују да су и брзина узорка и угао удара између абразивних честица и истрошене површине статистички значајни фактори који утичу на процес хабања и губитак масе премаза, при чему брзина има израженији утицај на губитак масе.